

Submitted to *Ap.J.Letters*, October 13, 2017

AGILE Observations of the Gravitational Wave Source GW170817: Constraining Gamma-Ray Emission from a NS-NS Coalescence

F. Verrecchia^{1,2}, M. Tavani^{3,4,5}, I. Donnarumma^{6,3}, A. Bulgarelli⁷, Y. Evangelista³,
L. Pacciani³, A. Ursi³, G. Piano³, M. Pilia⁹, M. Cardillo³, N. Parmiggiani⁷, A. Giuliani⁸,
C. Pittori^{1,2}, F. Longo¹⁰, F. Lucarelli^{1,2}, G. Minervini³, M. Feroci³, A. Argan³, F. Fuschino⁷,
C. Labanti⁷, M. Marisaldi¹⁷, V. Fioretti⁷, A. Trois⁹, E. Del Monte³, L.A. Antonelli¹,
G. Barbiellini¹⁰, P. Caraveo⁸, P.W. Cattaneo¹¹, S. Colafrancesco¹⁵, E. Costa^{3,6}, F.
D’Amico⁶, A. Ferrari¹², P. Giommi⁶, A. Morselli¹³, F. Paoletti^{19,3}, A. Pellizzoni⁹,
P. Picozza¹³, A. Rappoldi¹¹, P. Soffitta³, S. Vercellone¹⁴, L. Baroncelli⁷, G. Zollino⁷.

¹Space Science Data Center/ASI (SSDC), via del Politecnico, I-00133 Roma, Italy

²INAF-OAR, via Frascati 33, I-00078 Monte Porzio Catone (Roma), Italy

³INAF-IAPS, via del Fosso del Cavaliere 100, I-00133 Roma, Italy

⁴Dip. di Fisica, Univ.di Roma “Tor Vergata”, via della Ricerca Scientifica 1, I-00133 Roma, Italy

⁵Gran Sasso Science Institute, viale Francesco Crispi 7, I-67100 L’Aquila, Italy

⁶ASI, via del Politecnico snc, I-00133 Roma, Italy

⁷INAF-IASF-Bologna, via Gobetti 101, I-40129 Bologna, Italy

⁸INAF-IASF Milano, via E.Bassini 15, I-20133 Milano, Italy

⁹INAF, Osservatorio Astronomico di Cagliari, via della Scienza 5, I-09047 Selargius (CA), Italy

¹⁰Dip. di Fisica, Università di Trieste and INFN, via Valerio 2, I-34127 Trieste, Italy

¹¹INFN-Pavia, via Bassi 6, I-27100 Pavia, Italy

¹² CIFS, c/o Physics Department, University of Turin, via P. Giuria 1, I-10125, Torino, Italy

¹³INFN Roma Tor Vergata, via della Ricerca Scientifica 1, I-00133 Roma, Italy

¹⁴INAF, Osservatorio Astronomico di Brera, via Emilio Bianchi 46, I-23807 Merate (LC), Italy

¹⁵University of Witwatersrand, Johannesburg, South Africa

¹⁶Birkeland Centre for Space Science, Department of Physics and Technology, University of Bergen, Norway

¹⁷Unitat de Física de les Radiacions, Departament de Física, and CERES-IEEC, Universitat Autònoma de Barcelona, E-08193 Bellaterra, Spain

¹⁸East Windsor RSD, 25A Leshin Lane, Hightstown, NJ 08520 (USA)

ABSTRACT

The LIGO/Virgo Collaboration (LVC) detected on August 17, 2017 an exceptional gravitational wave (GW) event temporally consistent within ~ 2 s with the GRB170817A observed by *Fermi*/GBM and INTEGRAL. The event turns out to be compatible with a neutron star–neutron star (NS–NS) coalescence that subsequently produced a radio/optical/X-ray transient detected at later times.

We report the main results of the observations by the AGILE satellite of the GW170817 localization region (LR) and its electromagnetic counterpart. At the LVC detection time T_0 , the GW170817 LR was occulted by the Earth. The AGILE instrument collected useful data before and after the GW/GRB event because in its spinning observation mode it can scan a given source many times per hour. The earliest exposure of the GW170817 LR by the gamma-ray imaging detector (GRID) started about 935 s after T_0 . No significant X-ray or gamma-ray emission was detected from the LR that was repeatedly exposed over timescales of minutes, hours and days before and after GW170817, also considering Mini-Calorimeter and Super-AGILE data.

Our measurements are among the earliest ones obtained by space satellites on GW170817, and provide useful constraints on the precursor and delayed emission properties of the NS–NS coalescence event. We can exclude with high confidence the existence of an X-ray/gamma-ray emitting magnetar-like object with a large magnetic field of 10^{15} G. Our data are particularly significant during the early stage of evolution of the e.m. remnant.

Subject headings: gravitational waves, gamma rays: general.

1. Introduction

Automatic processing of *Fermi*/GBM data revealed on August 17, 2017 a low-fluence short gamma-ray burst (GRB) (now named GRB 170817A) detected in the 10–1000 keV range (Connaughton et al. 2017; von Kienlin et al. 2017; Goldstein et al. 2017). The LIGO/Virgo Collaboration (LVC) identified a very significant gravitational wave (GW) event preceding the GBM trigger by 2 seconds. Rapid communication of this double event was promptly issued (The LIGO Scientific Collaboration and Virgo Collaboration 2017a,b,c,d,e). GRB 170817A was soon confirmed by *INTEGRAL*/SPI-ACS (Savchenko et al. 2017a,c; Abbott et al. 2017e). This event (now named GW170817) is very relevant for several reasons. It is the first GW source detected in close temporal coincidence with a short GRB suggesting

a physical relation between the two events. It is the first detected gravitational event associated with a coalescence of two neutron stars. Furthermore, it is the second GW event for which Advanced Virgo (Acernese et al. 2015) could provide crucial constraints on the localization region restricting it to a few tens of square degree. These remarkable facts allowed, for the first time, to search for counterparts in an effective way (Abbott, & et al. 2017d, hereafter MMA17).

The event occurred at time $T_0 = 12:41:06.470$ UTC, (Abbott et al. 2017b, hereafter A17b). The event was identified by LVC as a compact binary coalescence (CBC) of two neutron stars (NSs) of total mass $2.82^{+0.47}_{-0.09} M_\odot$ and the individual masses in the range $0.86 - 2.26 M_\odot$. The estimated redshift of the system is $z = 0.008^{+0.002}_{-0.003}$ corresponding to a distance of 40^{+8}_{-14} Mpc (A17b). GW170817 is the first NS star coalescence candidate event with a “false-alarm rate” (FAR) less than one in 8.0×10^4 years as determined by a refined analysis (A17b). This event is the fifth of a set of confirmed GW events detected by LVC, GW150914 and GW151226 (Abbott et al. 2016a,b,c,d,e,f), GW170104 (Abbott et al. 2017a), and the more recent GW170814 (Abbott et al. 2017c), the first revealed using the Virgo detector data.

A first sky map of GW170817 was distributed through a LVC-GCN on August 17th, 2017 (The LIGO Scientific Collaboration and Virgo Collaboration 2017b), including an initial localization generated by the BAYESTAR pipeline (Singer & Price 2016) and based on data from the LIGO Hanford data only. An updated sky map was distributed about 10 hours later (The LIGO Scientific Collaboration and Virgo Collaboration 2017e), obtained using LALInference (Veitch et al. 2015), based on data from the three detectors LIGO Hanford, LIGO Livingston and Virgo. The source could be located in a sky region of 28 deg^2 (90% c.l.).

After the LVC announcement, a multi-wavelength campaign immediately started. The campaign involved the X and gamma-ray satellites first, and radio/IR-optical/TeV ground observatories at later times. The detection of a new optical transient (OT) was first announced by the One-Meter, Two-Hemisphere (1M2H) team discovered with the 1-m Swope telescope on Aug 18 01:05 UT (Coulter et al. 2017a,b; Drout et al. 2017), named Swope Supernova Survey 2017a (SSS17a, now with the IAU designation AT2017gfo). The OT was also detected independently by other five teams, the Dark Energy Camera (Allam et al. 2017; Cowperthwaite et al. 2017), the Distance Less Than 40 Mpc Survey (Yang et al. 2017; Valenti et al. 2017a; Tartaglia et al. 2017), Las Cumbres Observatory (Arcavi et al. 2017a,b,c), the Visible and Infrared Survey Telescope for Astronomy (Tanvir et al. 2017a,b), and MAS-TER (Lipunov et al. 2017a,b), REM-ROS2 (Melandri et al. 2017a,b; Pian et al. 2017), Swift UVOT/XRT (Evans et al. 2017a,b), and Gemini-South (Singer et al. 2017; Kasliwal et al.

2017), and for all see also MMA17. AT2017gfo is located at $10.6''$ from the early type galaxy NGC 4993, at a distance ~ 40 Mpc. A sequence of satellite high-energy observations started almost immediately, with exposures of the GW170817 LR depending on satellite position and operations. The X and γ -ray observations included contributions by CALET (Nakahira et al. 2017), Konus-Wind (Svinkin et al. 2017), Insight-HXMT (Liao et al. 2017), AstroSat CZTI (Balasubramanian et al. 2017), AGILE-GRID (see below), *Fermi*/LAT (Kocevski et al. 2017), MAXI (Sugita et al. 2017a,b), Super-AGILE (MMA17 and this paper), Swift X-Ray Telescope (Evans et al. 2017a,b), NuSTAR (Harrison et al. 2017), INTEGRAL JEM-X (Savchenko et al. 2017b,c), and Chandra (Margutti et al. 2017a; Troja et al. 2017a; Fong et al. 2017a). An X-ray counterpart detection at the OT position was reported after nine days and confirmed after fifteen days by Chandra (Troja et al. 2017a; Fong et al. 2017a; Margutti et al. 2017b; Troja et al. 2017b). Moreover an important detection in the radio band has been reported by VLA (Alexander et al. 2017a,b).

AGILE promptly reacted to the initial LVC notification of GW170817, and started a quicklook analysis as data became available within 1-2 hours as discussed below (Pilia et al. 2017; Piano et al. 2017; Bulgarelli et al. 2017; Verrecchia et al. 2017b).

The AGILE satellite that is in a equatorial orbit at an altitude of ~ 500 km (Tavani et al. 2009) is exposing 80% of the entire sky every 7 minutes in a “spinning mode”. The instrument consists of an imaging gamma-ray Silicon Tracker (sensitive in the energy range 30 MeV–30 GeV), Super-AGILE (SA, operating in the energy range 20–60 keV), and the Mini-Calorimeter (MCAL, working in the range 0.35 – 100 MeV; Labanti et al. 2009; Marisaldi et al. 2008; Fuschino et al. 2008) with an omni-directional field of view (FoV) and self-triggering capability in burst-mode for various trigger timescales. The anticoincidence (AC) system completes the instrument (for a summary of the AGILE mission features, see Tavani et al. 2009). The combination of Tracker, MCAL and AC working as a gamma-ray imager constitutes the AGILE-GRID. The instrument is capable of detecting gamma-ray transients and GRB-like phenomena on timescales ranging from sub-milliseconds to tens-hundreds of seconds.

The AGILE instrument has important characteristics for observations of large GW source LRs: a very large FoV of the GRID (2.5 sr); 80% of the whole sky that can be exposed every 7 minutes; 100–150 useful passes every day for any region in the accessible sky; a gamma-ray exposure of ~ 2 minutes of any field in the accessible sky every 7 min; sensitivity of $\sim 10^{-8}$ erg cm $^{-2}$ s $^{-1}$ above 30 MeV for typical single-pass of un-occulted sky regions; a sub-millisecond MCAL trigger for very fast events in the range 0.4–100 MeV; hard X-ray (18–60 keV) triggers of GRB-like events with a localization accuracy of 2-3 arcmin in the SA FoV (~ 1 sr) when operating in imaging mode.

Satellite data are transmitted to the ground currently on average every passage over the ASI Malindi ground station in Kenya and delivered to the AGILE Data Center (ADC; part of the ASI Space Science Data Center). Scientific data are then processed by a fast dedicated pipeline (AGILE GW, AGW), recently enhanced for the search of electromagnetic (e.m.) counterparts of GW sources. AGILE data processing can typically produce an alert for a transient gamma-ray source and/or GRB-like events within 20 min–2 hrs from satellite on-board acquisition depending on orbital and satellite parameters (Bulgarelli et al. 2014; Pittori 2013).

In this paper we present the main results of the analysis of AGILE data concerning GW170817. Sect. 2 presents the results on gamma-ray emission above 30 MeV from GW170817. Sect. 3 presents the results of Super-AGILE and MCAL observations. We discuss our measurements of GW170817 and their implications in Sect. 4.

2. Gamma-ray observations of GW170817

2.1. Prompt emission

The AGILE satellite was occulted by the Earth at the moment of the LVC detection. Therefore, there are no prompt data obtained by the GRID at the position of the OT. Fig. 1 shows the gamma-ray sensitivity map above 30 MeV at the GW170817 trigger time, with the Earth covering completely the GW170817 LR (obtained from the 90% LR extracted from the refined localization map; A17b). Since the AGILE satellite rotates every ~ 7 minutes around the axis pointed towards the Sun, the GRID obtained exposures of the GW170817 LR for each satellite revolution not affected by Earth occultation or SAA passages. We consider here three types of time intervals preceding and following the T_0 with different integration timescales: (a) short timescales, with 150 s integrations covering the interval $[-3100, +2900]$ s (times refer to T_0); (b) medium timescales, with integrations ranging from 1 hour to 1 day covering the interval $[-1, +1]$ day; (c) long timescales, with integrations ranging from 1 day to 50 days covering the interval $[-101, +21]$ days.

2.2. Early observations with short timescales

For the relatively short exposures during the first passes of the GW170817 LR we used the GRID "GRB detection mode", that maximizes the detection of relatively short gamma-ray transients lasting a few tens of seconds (as already applied to the short GRB 090510; Giuliani et al. 2010). We show in Fig. 3 the sequence of 150 s duration passes over the LR

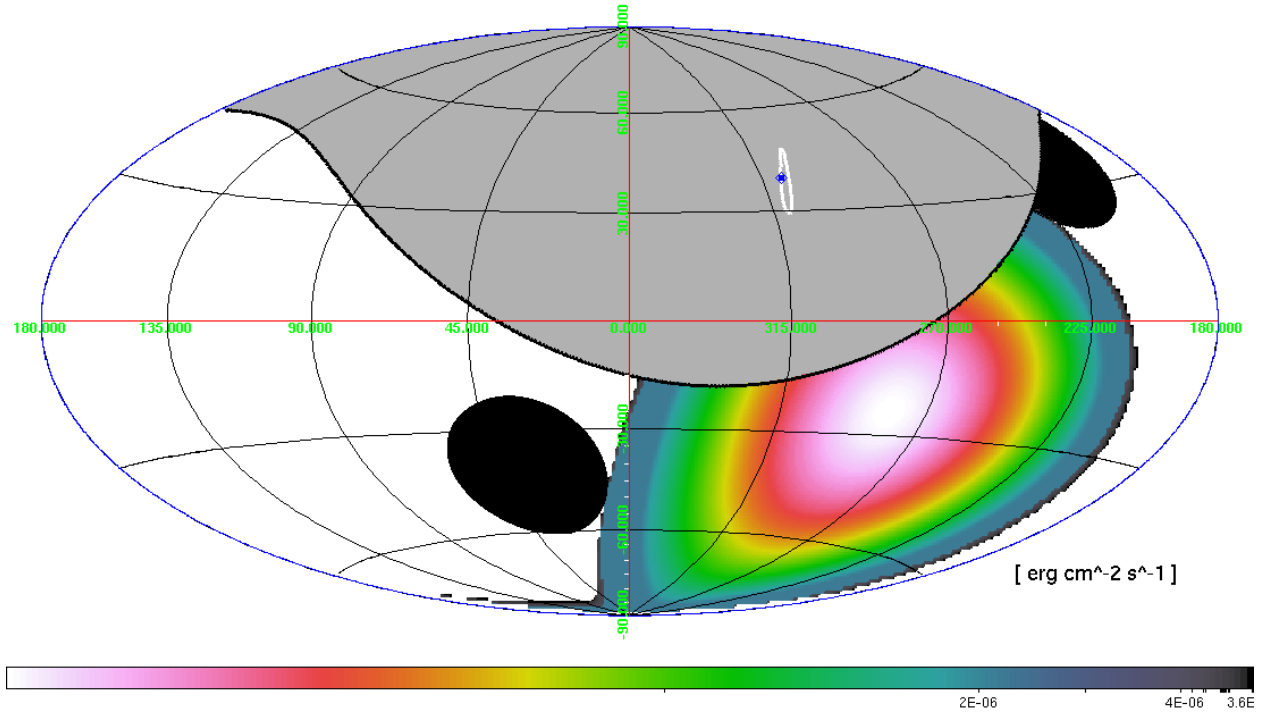


Fig. 1.— The AGILE-GRID $E > 30$ MeV UL map (in $\text{erg cm}^{-2}\text{s}^{-1}$ and Galactic coordinates) based on the gamma-ray 4 s exposure at the detection time T_0 of GW170817. The shadowed areas show the Earth-occulted region and the sky fraction not directly accessible by AGILE for solar panel constraints. The white contour shows the “preliminary LAL-Inference” 90% c.l. LR of GW170817 (The LIGO Scientific Collaboration and Virgo Collaboration 2017e) and the blue diamond marker is at the OT AT2017gfo position. The AGILE instrument does not have significant exposure of the LR at T_0 , which is covered by the Earth contour.

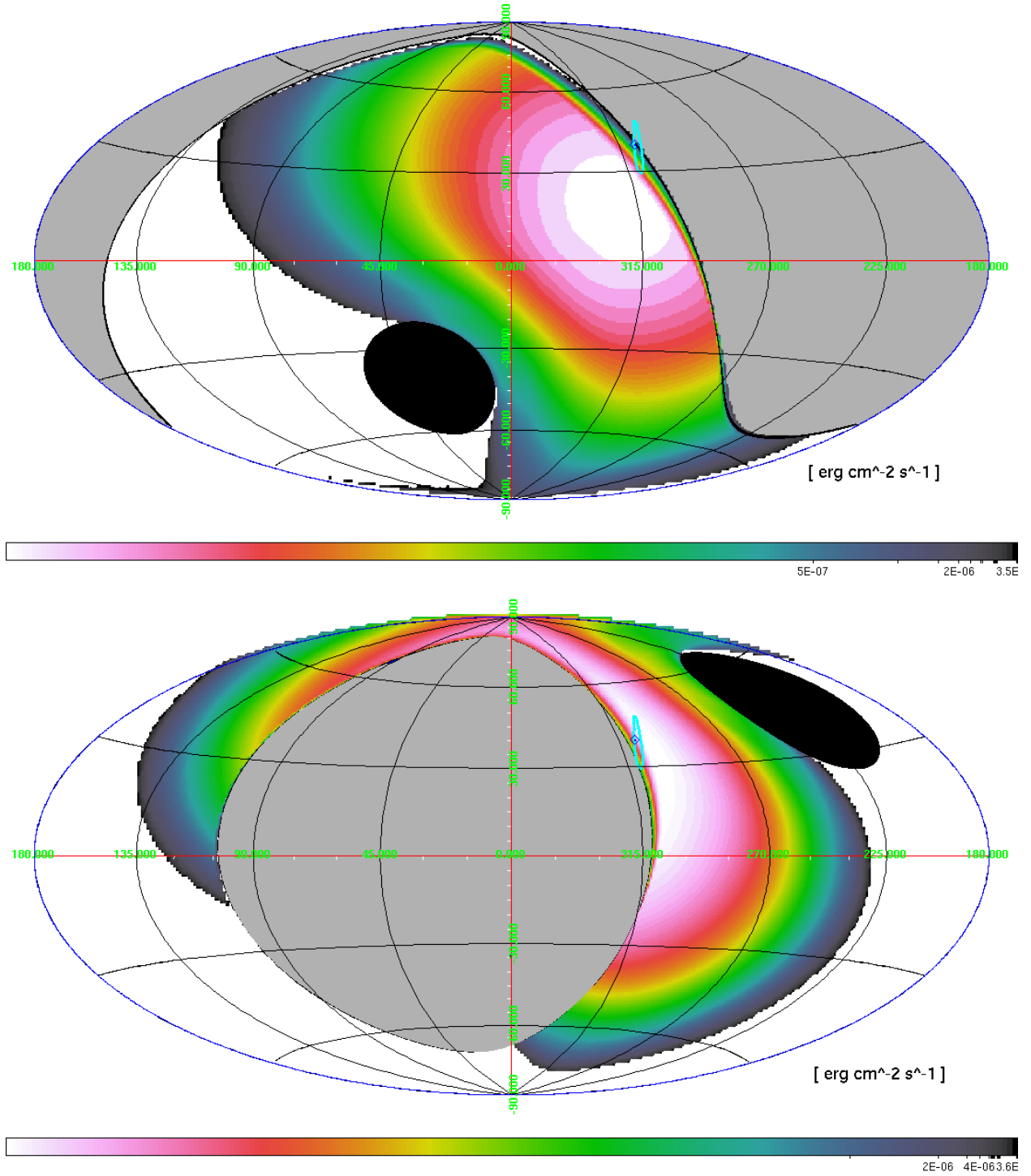


Fig. 2.— The AGILE-GRID $E > 30$ MeV UL maps (in $\text{erg cm}^{-2}\text{s}^{-1}$ and Galactic coordinates) for the 150 s exposures nearest to the T_0 , centered at -1260 and +1010s (times refers to T_0). The “preliminary LAL-Inference” 90% c.l. LR of GW170817 (The LIGO Scientific Collaboration and Virgo Collaboration 2017e) is shown in cyan color and the blue diamond marker is at the optical transient AT2017gfo position.

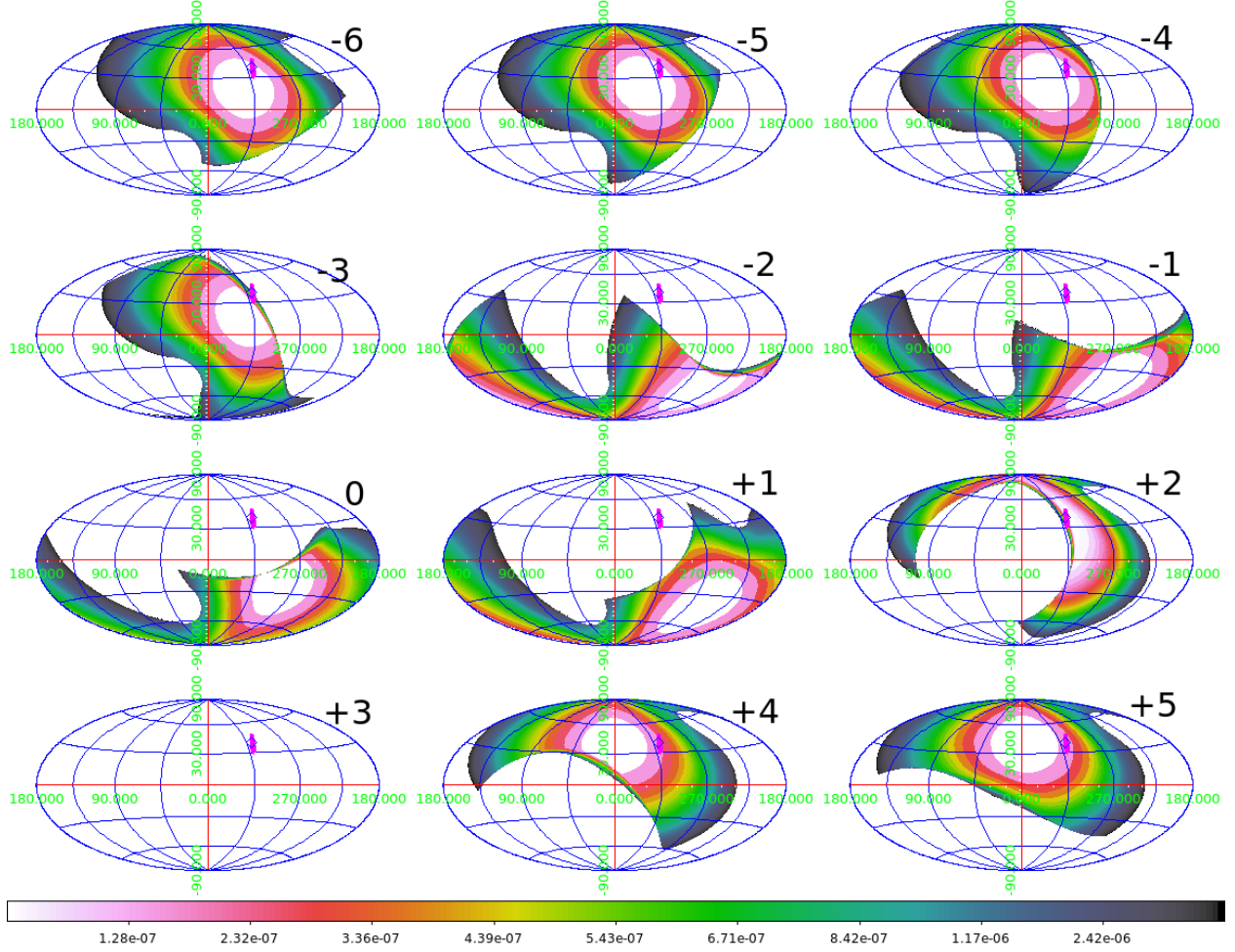


Fig. 3.— The AGILE-GRID sequence of 12 passes over the OT AT2017gfo obtained during the period $(-2813 \text{ s}, +2435 \text{ s})$ with respect to T_0 . The maps report the gamma-ray flux 3σ upper limits (in $\text{erg cm}^{-2}\text{s}^{-1}$) in the energy range 30 MeV - 10 GeV, with the lowest values at the OT AT2017gfo position being $UL = 1.9 \times 10^{-8} \text{ erg cm}^{-2} \text{ s}^{-1}$. The sequence shows all the 150 s integration maps for all the single spinning rotations reported in Table 1. The purple contour corresponds to the GW170817 LR according to the “preliminary LAL-Inference” 90% c.l. (The LIGO Scientific Collaboration and Virgo Collaboration 2017e), while the AT2017gfo position is marked with the blue diamond symbol.

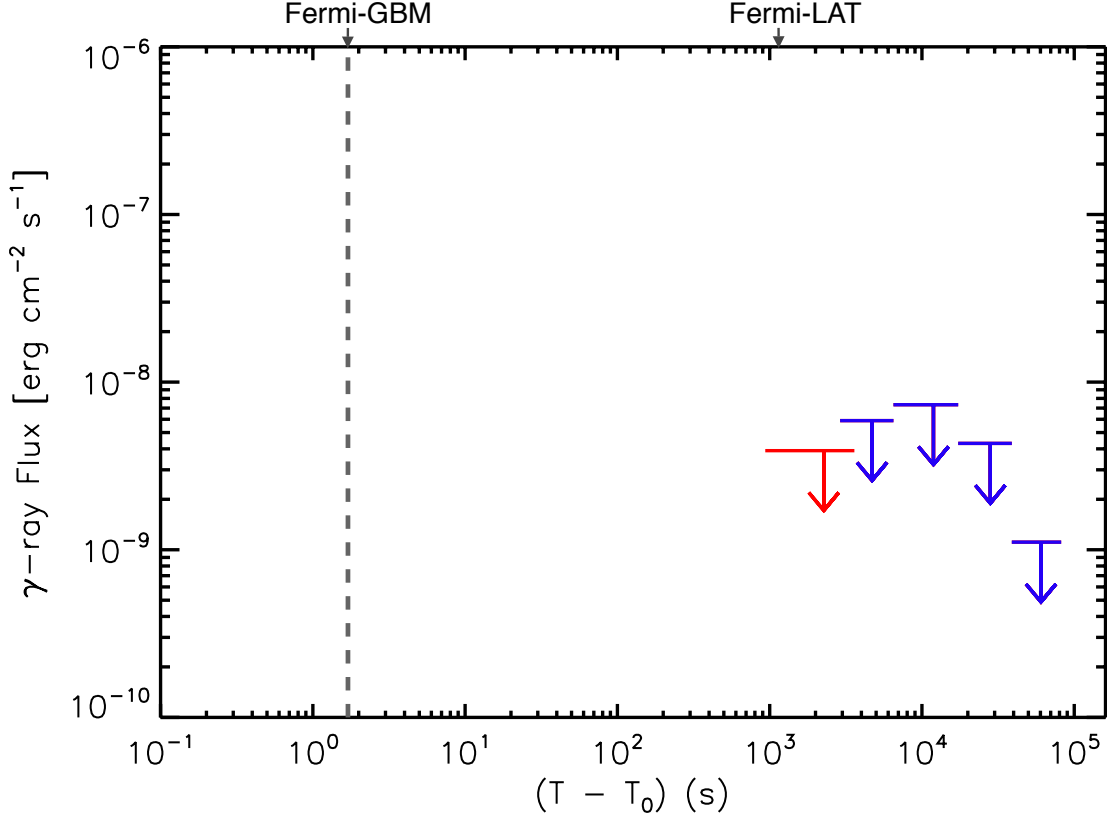


Fig. 4.— We show the AGILE-GRID gamma-ray 2-sigma ULs obtained at the AT2017gfo position and at different times with integrations of 2665 s, marked in red color, and integrations ranging from 1 to 12 hours, marked in blue color.

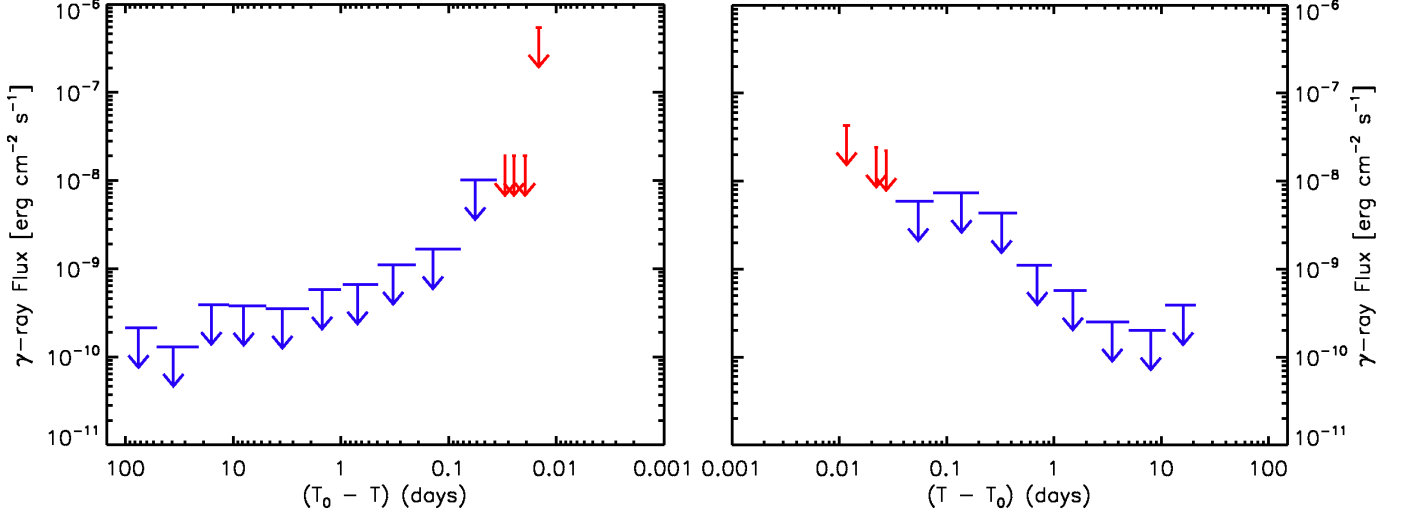


Fig. 5.— The AGILE-GRID gamma-ray 2-sigma ULs obtained at the OT AT2017gfo position at different times and integrations and derived L_{iso} considering the OT estimated redshift. Integrations of 150 s in the 30 MeV – 10 GeV band are marked in red color, while those ranging from 1 hour to 100 days in 100 MeV - 10 GeV are marked in blue color. On the left the ULs preceding T_0 till T_0-101 days, and on the right the ones following it till T_0+21 days.

within $-3100\text{ s} < t < +2900\text{ s}$, and we summarize in Table 1 the 2σ flux UL obtained at the OT position. We label time intervals of the highest GRID exposure with progressive numbers with respect to the prompt interval ΔT_0 . The intervals nearest in time to T_0 are the ΔT_{-3} and ΔT_{+2} ones. We then obtain 2σ flux upper limits in the 30 MeV – 10 GeV band, with 150 s integrations within the time interval $[-3100, +2900]$ s. The values for the integrations nearest in time to T_0 are: $UL_{-3} = 5.5 \times 10^{-7} \text{ erg cm}^{-2} \text{ s}^{-1}$ for the interval $[-1335, -1175]$ s, $UL_{+2} = 4.3 \times 10^{-8} \text{ erg cm}^{-2} \text{ s}^{-1}$ for the interval $[+935, +1085]$ s. For a 2665 s integration including the ΔT_{+2} interval we obtain: $UL_{2ks} = 3.9 \times 10^{-9} \text{ erg cm}^{-2} \text{ s}^{-1}$ for the overall time interval¹ $[+935, +3600]$ s. In Fig.4 we report our gamma-ray ULs obtained at the times reported in Table 1 with the indication of the GRB 170817A Fermi-GBM detection time and of the Fermi-LAT observation. No other gamma-ray observation of the GW170817 LR is available in the range 30 MeV - 30 GeV.

¹The integration time of 2665 s corresponds to a lower effective exposure time of ~ 400 s because of the satellite revolutions in spinning mode (see Table 1).

Table 1: Analysis of individual passes over the AT2017gfo position in the GRB-detection mode.

Interval number	Start time ^(*) [s]	Δt ^(**) [s]	2σ UL 30 MeV - 10 GeV [10^{-8} erg cm $^{-2}$ s $^{-1}$]	Comments
-6	-2663	150	1.9	LVC source occulted by the Earth LVC source occulted by the Earth LVC source occulted by the Earth LVC source occulted by the Earth excluded due to SAA passage
-5	-2213	150	1.9	
-4	-1763	150	1.9	
-3	-1335	150	54.5	
-2	-1013	150	—	
-1	-563	150	—	
0	0	150	—	
+1	+335	150	—	
+2	+935	150	4.3	
+3	+1385	150	—	
+4	+1835	150	2.4	
+5	+2285	150	2.2	
—	-3100	3100	0.6	
—	+0	2900	0.5	

^(*)Start time of the time interval with respect to T_0 , $t - T_0$, in seconds. ^(**) Integration time in s. ^(***) 2σ flux upper limit obtained with the “GRB detection mode” for emission at the AT2017gfo position with integrations of 150 s except for the last two rows obtained with exposures of 3100 and 2900 s before and after T_0 .

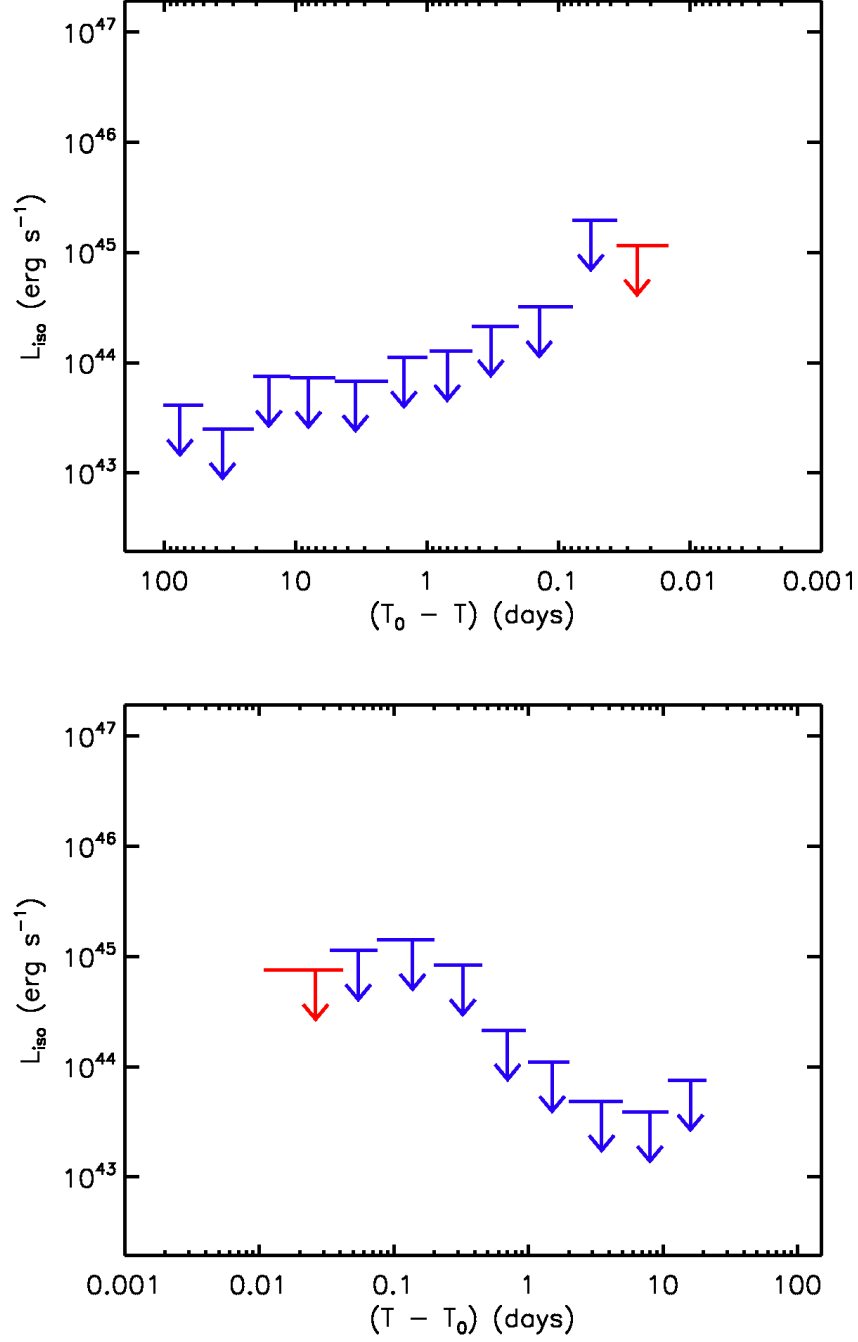


Fig. 6.— The AGILE-GRID sequence of ULs converted into luminosity limits (in erg s^{-1}) considering the OT distance of 40 Mpc, obtained at times preceding and following T_0 with integration times of 2665 s (top panel) and 1915 s marked in red color, and ranging from 1 hour to 50 days in blue. All GRID upper limits were obtained at the AT2017gfo position.

Table 2: Analysis of GRID data over medium-timescale integration times at the OT AT2017gfo position.

Interval number	Start time ^(*) [ks]	Δt (**) [hr]	2σ UL (***) [10^{-9} erg cm $^{-2}$ s $^{-1}$]
-10	-32.9	12	0.66
-9	-11.3	6	1.11
-8	-6.7	3	1.66
-7	-3.1	1	10.07
+6	+2.9	1	5.89
+7	+6.5	3	7.33
+8	+17.3	6	4.31
+9	+38.9	12	1.11
–	-86.4	24	0.55
–	+0	24	1.47

^(*) Start time of the interval with respect to T_0 , $t - T_0$, in ks. The second table part reports the UL on integrations on the total time covering all the pre/post- T_0 intervals. ^(**) Integration time in hours. ^(***) 2σ flux upper limit (10^{-9} erg cm $^{-2}$ s $^{-1}$) obtained for emission in the range 100 MeV - 10 GeV with the AGILE Maximum Likelihood analysis at the AT2017gfo position.

2.3. Search for precursor and delayed gamma-ray emission

AGILE was uniquely able to collect data on the GW170817 LR during selected time intervals preceding and following the prompt event. We carried out a search for transient gamma-ray emission on integrations smaller than one day (see Tab. 2.2) during the hours and days immediately following or preceding the prompt event (see Fig. 5). Finally we performed also a search on longer timescales up to one hundred days before and twenty days after the event. Table 2.3 summarizes our results and upper limits for these long integrations. No significant gamma-ray emission in the GW170817 LR was detected over integrations of hours up to 50 days at covering times from $T_0 - 101$ days to $T_0 + 21$ days.

The long timescale GRID data analysis included two further searches for transient gamma-ray detections with equal integrations of 1000s, 12 hours, 1 and 2 days. In particular, we have performed a search for gamma-ray emission from August 1, 2017, to August 31, 2017, at 1000 s integration timescale. On August 24, 2017, 09:31:39 UTC, using the method described in Li & Ma (1983) we detected a weak gamma-ray source apparently coincident with the GW170817 OT at 4.2σ pre-trial significance. Our analysis leads to a

Table 3: Long time scale integration times analysis at the OT position.

Interval number	Start time ^(*) [days]	Δt ^(**) [days]	2σ UL ^(***) [10^{-10} erg cm $^{-2}$ s $^{-1}$]
-16	-101	50	2.12
-15	-51	30	1.30
-14	-21	10	3.88
-13	-11	6	3.80
-12	-5	3	3.52
-11	-2	1	5.79
+10	+1	1	5.71
+11	+2	3	2.52
+12	+5	6	2.01
+13	+11	10	3.88

^(*)Start time of the interval with respect to T_0 , $t - T_0$, in days. ^(**) Integration time in days. ^(***) 2σ flux upper limit (10^{-10} erg cm $^{-2}$ s $^{-1}$) obtained for emission in the range 100 MeV - 10 GeV with the AGILE Maximum Likelihood analysis at the AT2017gfo position and for a mean power law spectrum with photon index -2.

marginal post-trial significance of 3.1σ for this source. Similar searches on 1 and 2 days integration timescales over $[-10, +10]$ days time interval have been performed discarding low exposure integrations, and executing the AGILE maximum likelihood analysis (Mattox et al. 1996; Bulgarelli et al. 2012) at the OT position. Another low-significance source apparently coincident with the OT is found in a 1-day integration starting at August 9, 00:00:00 UTC, with a pre-trial significance of 3.3σ .

3. Super-AGILE and MCAL observations

The Super-AGILE detector (Feroci et al. 2007) observed the location of GW170817 starting at 2017-08-18 01:16:34.84 UTC, that is with a $\Delta t = 0.53$ days with respect to the LVC trigger time restarting its science observations after a 12-hour period of "idle mode", due to telemetry-saving requirements at mission level. We report here the analysis for the first available orbit after the idle time interval. The location of GW170817 crossed thus the FoV of the Super-AGILE detector at 23.5 deg off-axis in one coordinate (X), while scanning the entire FoV in the orthogonal coordinate (Y). This is a rather unfavourable viewing angle for SA, greatly reducing its effective area and sensitivity thereof. We restricted our analysis

between -15 deg and +15 deg in the Y-coordinate, exposing on average 32% of the peak effective area. The observation of the GW source is composed by a set of 15 time intervals (one per satellite rotation), each one lasting about 40 s, for a total net exposure time of 573 s. No X-ray source was detected at the location of GW 170817, with a 3-sigma upper limit in the 18-60 keV energy band of $3.0 \times 10^{-9} \text{ erg cm}^{-2} \text{ s}^{-1}$.

As the OT is de-occulted and accessible by MCAL near +935 s, we obtain flux ULs with the MCAL detector at times -1328 s and +1023 s. No evidence of triggered or untriggered significant emission detected by MCAL was measured. We obtained a 2- σ fluence UL in the energy band 400 keV - 100 MeV, $UL = 3.1 \times 10^{-7} \text{ erg cm}^{-2}$ at times -1328 s and +1023 s, using a power law model with a photon index of 1.4.

4. Discussion and Conclusions

AGILE contributed in a significant way to the multifrequency follow-up observations of the exceptional event GW170817 (MMA17). Despite the Earth occultation of the LR at T_0 , AGILE obtained very relevant X-ray and gamma-ray constraints on GW170817. As reported in Bulgarelli et al. (2017) and MMA17, the earliest gamma-ray imaging detector data were obtained near $T_1 = +935$ s. Table 1 and Fig. 3 show the results of the first useful passes over the GW170817 LR. Of particular relevance to our discussion is the upper limit to gamma-ray emission above 30 MeV obtained with an integration of about 2600 s after T_1 , $F_\gamma = 3.9 \times 10^{-9} \text{ erg cm}^{-2} \text{ s}^{-1}$. For a distance $d = 40$ Mpc this translates in a limiting isotropic gamma-ray luminosity $L_{iso\gamma} = 7.8 \cdot 10^{44} \text{ erg s}^{-1}$. It is interesting to note that the peak isotropic luminosity of GRB170817A in the 10-1000 keV band detected by *Fermi*/GBM is $L_{iso,GBM} \simeq 6 \cdot 10^{46} \text{ erg s}^{-1}$ (Goldstein et al. 2017; Abbott et al. 2017e, MMA17). Figs. 3 and 5 show the overall trend of the gamma-ray upper limits obtained by the AGILE-GRID at later times. In terms of upper limits of the gamma-ray luminosity, the results of Fig. 6 indicate a range of isotropic luminosities between 10^{43} and $10^{45} \text{ erg s}^{-1}$. Furthermore, the imaging Super-AGILE provided one of the earliest upper limits to hard X-ray emission in the band 18–60 keV at $\Delta t = 0.53$ d (see also Table 4 of MMA17), $F_X < 3 \cdot 10^{-9} \text{ erg cm}^{-2} \text{ s}^{-1}$ that translates into a limiting isotropic luminosity of $L_{iso,X} = 5.8 \cdot 10^{44} \text{ erg s}^{-1}$. We note that both GRID and Super-AGILE provide similar limits to the emitted luminosity in their different energy bands even though at different times (+0.011 days and +0.53 days, respectively). The non-imaging MCAL provided data as the GW170817 LR was de-occulted by the Earth. Assuming the same spectral model applicable to GRB170817A (MMA17), the 90% c.l. fluence upper limit is $F_{MCAL} < 3 \cdot 10^{-7} \text{ erg cm}^{-2}$, that turns out to be similar to other measurements by other calorimetric detectors (see Table 3 of MMA17).

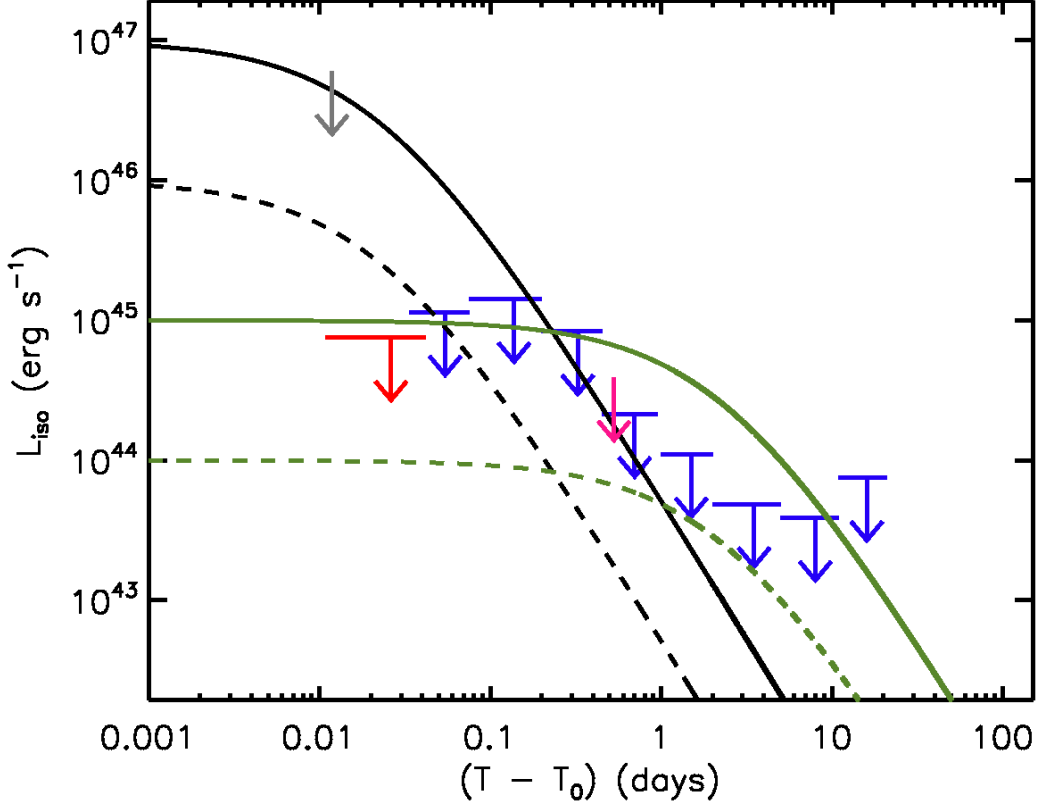


Fig. 7.— AGILE 2- σ ULs obtained from observations of the GW170817 localization region and converted into luminosity limits (in erg s^{-1}) for an OT distance of 40 Mpc. In blue color we show the AGILE-GRID ULs in the energy range 100 MeV – 10 GeV. In red color we show the early GRID UL in the range 30 MeV – 10 GeV. Marked in purple and gray colors are the Super-AGILE and MCAL flux ULs in the 18–60 keV and 400 keV – 100 MeV bands, respectively. We also show the high-energy luminosity curves relative to the magnetar-like remnant model described in Section 4. The black lines refer to a model with a poloidal magnetic field $B_p = 10^{15}$ G and a radiation efficiencies ξ of 10^{-2} (solid line) and 10^{-3} (dashed line). Green lines correspond to a model with $B_p = 10^{14}$ G and $\xi = 10^{-2}$ (solid) or $\xi = 10^{-3}$ (dashed).

The limiting luminosities implied by our measurements can be interpreted in a context of high-energy radiation possibly emitted by either an expanding fireball/jet, or by a remnant left over of the NS-NS coalescence. The latter hypothesis is more interesting in terms of constraints that can be obtained by the AGILE-GRID observations. If the remnant is a magnetar-like system loaded with a residual magnetic field and rapidly rotating (e.g. Usov 1992; Duncan & Thompson 1992; Thompson 1994; Spruit 1999; Zhang & Meszaros 2001) we can constrain its magnetic field assuming initial millisecond spin periods. The electromagnetic emission (EM) by magnetic dipole radiation of a star of radius R with a poloidal magnetic field B_p and angular frequency $\Omega = 2\pi/P$ (with P the spin period) is $L(t) = B_p^2 R^6 \Omega(t)^4 / 6c^3$ (with c the speed of light). Neglecting GW radiation at late times after coalescence, integration of the energy loss equation leads to the dependence of Ω as a function of time, $\Omega(t) = \Omega_0(1 + t/\tau)^{-1/2}$, with Ω_0 the initial frequency, and $\tau = 3c^3 I / (B_p^2 R^6 \Omega_0^2) \simeq (2 \cdot 10^3 \text{ s}) I_{45} B_{p,15}^{-2} P_{0,-3}^2 R_6^{-6}$, where I_{45} is the compact object moment of inertia in units of 10^{45} g cm^2 , $B_{p,15} = B_p / 10^{15} \text{ G}$, $P_{0,-3}$ is the initial spin period in units of 10^{-3} s , and R_6 is the radius of the compact object in units of 10^6 cm . For the EM-dominated regime of energy loss, we obtain the temporal behavior of the spin-down luminosity (e.g., Zhang and Meszaros 2001) $L_{sd}(t) = L_0 / (1 + t/\tau)^2$, with $L_0 = I \Omega_0^2 / (2\tau) \simeq (10^{49} \text{ erg s}^{-1}) B_{p,15}^2 P_{0,-3}^{-4} R_6^6$. It is interesting to note that in the absence of absorption effects, the radiated luminosity (in first approximation assumed here to be isotropic) has the limiting behavior, $L_{sd} = L_0$ for $t \ll \tau$, and $L_{sd} = L_0 (t/\tau)^{-2}$ for $t \gg \tau$. In our case, we can assume the remnant of radius $R_6 = 1$, moment of inertia $I_{45} = 1$ to rotate with an initial millisecond spin period, $P_{0,-3} = 1$. We then have the critical time τ depending only on the surface magnetic field $\tau \simeq (2 \cdot 10^3 \text{ sec}) B_{p,15}^{-2}$.

Assuming a conversion of spin-down luminosity $L_{sd}(t)$ into radiation by a factor ξ , we show the radiated luminosity $L_{rad}(t) = \xi L_{sd}(t)$ in Fig.7 under the assumptions of two different values of the poloidal magnetic field $B_p = 10^{15} \text{ G}$ and 10^{14} G , for two values of the conversion factors, $\xi = 10^{-2}$ and $\xi = 10^{-3}$. We denote by ξ the possibly different conversion efficiencies into hard X-rays and the GRID energy range above 30 MeV. We show in Fig. 7 all AGILE upper limits (from MCAL, Super-AGILE and GRID) together with the temporal behavior of high-energy radiation expected from a rapidly rotating magnetar. We see that the early AGILE-GRID upper limits are important in general, and in particular exclude highly magnetized magnetars. We see in Fig. 7 that magnetars models with $B_p = 10^{15} \text{ G}$ are excluded by the earliest GRID upper limit with high confidence also for $\xi = 10^{-3}$. Analogously, models with $B_p = 10^{14} \text{ G}$ are excluded for $\xi = 10^{-2}$.

Constraining the gamma-ray emission of GW170817 at early times (within the first few thousand seconds) is relevant also to models of possible magnetic field reconnection following the formation of a black hole. Transient gamma-ray emission can be expected

from the collapse of the coalescing NSs into a newly born black hole. We exclude models envisioning gamma-ray luminosities near $10^{45} \text{ erg s}^{-1}$ at +1000 s after coalescence.

AGILE continues to operate nominally, and will continue to observe the high-energy sky in the search for transient events associated with gravitational wave events.

This work is part of the multifrequency observation campaign of GW170817 whose main results are summarized in the Multi-Messenger-Astronomy (MMA) paper. We warmly thank our LIGO/Virgo and MMA collaborators for sharing information on the event and follow-up observations.

AGILE is an ASI space mission developed with programmatic support by INAF and INFN. We thank INAF and ASI for support. We acknowledge partial support through the ASI grant no. I/028/12/2.

REFERENCES

- Aasi, J., et al. (LIGO Scientific Collaboration), 2015, *Class. Quantum Grav.*32, 074001, 1411.4547.
- Acernese, F., et al. (Virgo Collaboration), 2015, *Class. Quantum Grav.*32, 024001, 1408.3978.
- Abbott, B. P., Abbott, R., Abbott, T. D., et al. 2016a, *Physical Review D*, 93, 122003
- Abbott, B. P., Abbott, R., Abbott, T. D., et al. 2016b, *Physical Review Letters*, 116, 131103
- Abbott, B. P., Abbott, R., Abbott, T. D., et al. 2016c, *Physical Review Letters*, 116, 241103
- Abbott, B. P., Abbott, R., Abbott, T. D., et al. 2016d, *Physical Review Letters*, 116, 061102
- Abbott, B. P., Abbott, R., Abbott, T. D., et al. 2016e, *Physical Review D*, 93, 122004
- Abbott, B. P., Abbott, R., Abbott, T. D., et al. 2016f, *Physical Review Letters*, 116, 241102
- Abbott, B. P., Abbott, R., Abbott, T. D., et al. 2017a, *Physical Review Letters*, 118, 221101
- Abbott, B. P., et al., 2017b, *Physical Review Letters*, accepted, doi:10.1103/PhysRevLett.119.161101 (A17b)
- . 2017c, *Physical Review Letters*, in press

- . 2017d, *ApJL*, in press, doi:10.3847/2041-8213/aa91c9 (MMA17)
- . 2017e, *ApJL*, in preparation, doi:10.3847/2041-8213/aa920c (LVC-GBM-INTEGRAL)
- Abdo, A. A., Ackermann, M., Ajello, M., et al. 2009, *Nature*, 462, 331
- Ackermann, M., Ajello, M., Albert, A., et al. 2016, *ApJL*, 823, L2
- Alexander, K., et al. 2017a, GRB Coordinates Network, 21538
- Alexander, K., et al. 2017b, *ApJSS*, in press
- Allam, S., Annis, J., Berger, E., Brout, D.J., Brown, D., et al., 2017, GRB Coordinates Network, 21530
- Arcavi, I., et al. 2017b, *ApJL*, in preparation
- Arcavi, I., et al. 2017c, *Nature*, in press, doi:10.1038/nature24291
- Arcavi, I., et al. 2017a, GRB Coordinates Network, 21538
- Balasubramanian, A., Mate, S., Bhalerao, V., et al. 2017, GRB Coordinates Network, 21514
- Bulgarelli, A., Chen, A.W., Tavani, M., et al., 2012, *A. & A.*, 540, A79
- Bulgarelli, A., Trifoglio, M., Gianotti, F., et al. 2014, *ApJ*, 781, 19
- Bulgarelli, A., Tavani, M., Verrecchia, F., Cardillo, M., Piano, G., et al. 2017, GRB Coordinates Network, 21564
- Connaughton, Blackburn, Briggs, et al., Connaughton, V., Blackburn, L., Briggs, M.S., et al., 2017, GRB Coordinates Network, 21506
- Coulter, D.A., Kilpatrick, C.D., Siebert, M.R., et al., 2017a, GRB Coordinates Network, 21529
- Coulter, D.A., et al. 2017b, *ApJL*, in preparation
- Cowperthwaite, P.S., et al. 2017, *ApJL*, accepted
- Del Monte, E., Barbiellini, G., Donnarumma, I., et al. 2011, *A&A*, 535, A120
- Drout, M.R., Coulter, D.A., et al., 2017, *ApJL*, in preparation
- Duncan, R.C., and Thompson, C., 1992, *ApJ*, 392, L9

- Evans, P., Cenko, B., Kennea, J.A., et al., 2017b, *Science*, submitted
- Evans, P., Cenko, B., Kennea, J.A., et al., 2017a, GRB Coordinates Network, 21612
- Feroci, M., Costa, E., Soffitta, P., et al., 2009, *Nuclear Instruments and Methods in Physics Research A*, 598, 470
- Fong, W., Margutti, R., Haggard, D., et al. 2017b, GRB Coordinates Network, 21786
- Fuschino, F., Labanti, C., Galli, M., et al. 2008, *Nuclear Instruments and Methods in Physics Research A*, 588, 17
- Galli, M., Marisaldi, M., Fuschino, F., et al. 2013, *A. & A.*, 553, A33
- Giuliani, A., Fuschino, F., Vianello, G., et al. 2010, *ApJ*, 708, L84
- Giuliani, A., Longo, F., Verrecchia, F., et al. 2013, GRB Coordinates Network, 15479
- Giuliani, A., Mereghetti, S., Fornari, F., et al. 2008, *A&A*, 491, L25
- Giuliani, A., Mereghetti, S., Marisaldi, M., et al. 2014, *ArXiv e-prints*
- Goldstein, A., et al., 2017, *ApJL*, 848, in press, doi:10.3847/2041-8213/aa8f41
- Harrison, F.A., Forster, K., Garcia, J., et al. 2017, GRB Coordinates Network, 21626
- Kasliwal, M., et al., 2017, *Science*, submitted
- Kocevski, D., Omodei, N., Buson, S., et al., 2017, GRB Coordinates Network, 21534
- Labanti, C., Marisaldi, M., Fuschino, F., et al. 2009, *Nuclear Instruments and Methods in Physics Research A*, 598, 470
- Li, T. & Ma, Y. 1983, *ApJ*, 272, 317
- Li, T.P., Xiong, S.L., Zhang, S.N., et al. 2017, *Science China Physics, Mechanics & Astronomy*, doi:10.1007/s11433-017-9107-5
- Liao, J.Y., Li, C.K., Ge, M.Y., et al. 2017, GRB Coordinates Network, 21518
- Lipunov, V.M., Gorbovskoy, E., Kornilov, V.G., Tyurina, N., Shumkov, V., et al. 2017a, GRB Coordinates Network, 21546
- Lipunov, V.M., et al., 2017b, *ApJL*, in press, doi:10.3847/2041-8213/aa92c0
- Longo, F., Giuliani, A., Marisaldi, M., et al. 2013, GRB Coordinates Network, 14344

- Longo, F., Moretti, E., Nava, L., et al. 2012, *A. & A.*, 547, A95
- Margutti, R., et al., 2017b, *ApJL*, in press
- Margutti, V., Fong, C., Berger, E., et al. 2017a, GRB Coordinates Network, 21648
- Marisaldi, M., Fuschino, F., Tavani, M., et al. 2014, *Journal of Geophysical Research (Space Physics)*, 119, 1337
- Marisaldi, M., Labanti, C., Fuschino, F., et al., 2008, *A&A*, 490, 1151
- Mattox, J.R., Bertsch, D.L., Chiang, J., et al. 1996, *ApJ*, 461, 396.
- Melandri, A., Campana, S., Covino, S., et al., 2017a, GRB Coordinates Network, 21532
- Melandri, L., et al., 2017b, *ApJL*, accepted
- Moretti, E., Longo, F., Barbiellini, G., et al. 2009, GRB Coordinates Network, 9069
- Nakahira, S., Yoshida, A., Sakamoto, T., et al., 2017, GRB Coordinates Network, 21641
- Pian, E., D’Elia, V., Piranomonte, F., et al. 2017, GRB Coordinates Network, 21592
- Pian, E., et al., 2017, *Nature*, in press
- Piano, G., Verrecchia, F., Pilia, M., Cardillo, C., Tavani, M., et al. 2017, GRB Coordinates Network, 21526
- Pilia, M., Cardillo, C., Piano, G., Tavani, M., Verrecchia, F., et al. 2017, GRB Coordinates Network, 21525
- Pittori, C. 2013, *Nuclear Physics B Proceedings Supplements*, 239, 104
- Melandri, A., Campana, S., Covino, S., et al., 2017, GRB Coordinates Network, 21532
- Singer, L. P. & Price, L. R. 2016, *Physical Review D*, 93, 024013
- Savchenko, V., Mereghetti, S., Ferrigno, C., et al. 2017a, GRB Coordinates Network, 21507
- Savchenko, V., Ferrigno, C., Bozzo, E., et al. 2017b, GRB Coordinates Network, 21672
- Savchenko, V., et al. 2017c, *ApJL*, in preparation
- Spruit, H.C., 1999, *A&A*, 341, L1
- Svinkin, D., Golenetskii, S., Aptekar, R., et al., 2017, GRB Coordinates Network, 21746

- Sugita, S., Kawai, N., Negoro, H., et al., 2017b, PASJ, in preparation
- Sugita, S., Kawai, N., Serino, M., et al. 2017a, GRB Coordinates Network, 21555
- Tanvir, L., et al., 2017b, ApJL, accepted
- Tartaglia, L., et al., 2017, ApJL, in preparation
- Tavani, M., Barbiellini, G., Argan, A., et al. 2009, A&A, 502, 995
- Tavani, M., Marisaldi, M., Labanti, C., et al. 2011, Physical Review Letters, 106, 018501
- Tavani, M., Pittori, C., Verrecchia, F., et al. 2016, ApJ, 825, L4
- Tanvir, S., Levan, S., et al. 2017a, GRB Coordinates Network, 21544
- Thompson, C., 1994, MNRAS, 270, 480
- The LIGO Scientific Collaboration and Virgo Collaboration. 2017a, GRB Coordinates Network, 21505
- The LIGO Scientific Collaboration and Virgo Collaboration. 2017b, GRB Coordinates Network, 21509
- The LIGO Scientific Collaboration and Virgo Collaboration. 2017c, GRB Coordinates Network, 21510
- The LIGO Scientific Collaboration and Virgo Collaboration. 2017d, GRB Coordinates Network, 21513
- The LIGO Scientific Collaboration and Virgo Collaboration. 2017e, GRB Coordinates Network, 21527
- Troja, E., Piro, L., Sakamoto, T., et al. 2017a, GRB Coordinates Network, 21765
- Troja, E., et al., 2017b, Nature, accepted, doi:10.1038/nature24290
- Usov, V.V., 1992, Nature, 357, 472
- Valenti, S, et al. 2017a, ApJL, accepted
- Veitch, J., Raymond, V., Farr, B., et al. 2015, Physical Review D, 91, 042003
- Verrecchia, F., Tavani, M., Ursi, A., et al. 2017a, ApJ, 847, L20

- Verrecchia, F., Cardillo, M., Bulgarelli, A., Tavani, M., Piano, G., et al. 2017b, GRB Coordinates Network, 21785
- Verrecchia, F., Pittori, C., Giuliani, A., et al. 2013, GRB Coordinates Network, 14515
- von Kienlin, Meegan, Goldstein, et al., von Kienlin, A., Meegan, C., Goldstein, A., et al., 2017, GRB Coordinates Network, 21520
- Yang, S., Valenti, S., Sand, D., Tartaglia, L., Cappellaro, E., et al. 2017a, GRB Coordinates Network, 21531
- Zhang, B., and Meszaros, P, 2001, ApJ, 552, L35